NONLINEAR ANALYSES OF COMPOSITE PREFLEX STEEL BEAMS ENCASED IN CONCRETE

Dr. Raad K. Al-Azawi
Lecturer. /Civil Eng. Dept.
College of Eng. / University of Baghdad.

Yousif S. Jafar
Master research student /Civil Eng. Dept.
College of Eng. / University of Baghdad.

ABSTRACT:

In the present study, a nonlinear three-dimensional finite element analysis has been used to predict the load-deflection and moment-rotation behaviors of composite encased beams consisting of preflex steel sections using the finite element computer program (**ANSYS V. 10**). Composite encased beams are analyzed and a comparison is made with available experimental moment-rotation curves, good agreement with the experimental results is observed. Camber of steel section is introduced on the steel section of the composite beams encased in concrete. It is found that using of preflex section can increase the ultimate load capacity of the composite encased beam by relatively (15%) and also it is found that rotations are nearly (65% to 80%) the rotations of the same beam without preflex steel section. Parametric studies have been carried out to study the increasing of the moment-carrying capacity due to the use of encased concrete for the laminated partially encased beams; meanwhile the slip along the composite partially encased beams length is studied. The strain distributions along the steel section and encased concrete depth are also examined. Poisson's ratio of concrete, the effect of cambering of steel-section and the effect of mesh refinement are also investigated.

KEYWORDS: Concrete Encasement, Finite Element Analyses, ANSYS Computer Program, Preflexing, Headed Studs.

الخلاصة:

أستخدم في الدراسة الحالية، طريقة العناصر المحددة للتحليل اللاخطي ثلاثي الابعاد و ذلك لغرض تحري علاقة منحنى كل من الحمل – الهطول و كذلك العزم – الدوران للعتبات المركبة و التي تحتوي على عنصر فولاذي مثني مغلف بالخرسانة وباستخدام برنامج العناصر المحددة للتحليل الانشائي الـ(**ANSYS V. 10**). تم تحليل العتبات المركبة ذوات المقاطع المغلفة و تمت مقارنة نتائج منحنيات العزم –الدوران مع النتائج العملية المتوفرة، تم ملاحظة توافق جيد بين النتائج المستحصلة من البرنامج و النتائج العملية. تم توليد تحديب (أنثناء) في المقطع الفولاذي للعتبات المركبة المغلفة بالخرسانة. لقد لوحظ بأن استخدام المقاطع المثنية في العتبات المركبة و المغلفة بالخرسانة يؤدي الى زيادة قابلية تحمل تلك العتبات بمقدار (١٥٪)، و كذلك لوحظ بأن الدوران يتراوح مابين (٦٥٪ الى ٨٠٪) من الدوران للعتبات التي تحتوي على مقاطع مثنية. تم دراسة تأثير وجود الخرسانة المغلفة على زيادة قابلية تحمل العزوم للعتبات القشرية المركبة و المغلفة جزئياً بالخرسانة، في تلك الاثناء تم دراسة التزحلق الذي يحدث في سطح الاتصال و على طول العتب للعتبات المركبة أيضاً. بالاظافة الى ذلك تم دراسة نمطية توزيع الانفعالات على العمق الكامل للمقاطع الفولاذية و كذلك الخرسانة المغلفة. و اخيراً، تم التحقق من تاثير كل من (Poisson's ratio)، مقدار تحدب (ثني) المقطع الفولاذي و مقدار نعومة (دقة) النموذج المعمول بالـ(**ANSYS**) على قابليات تحمل العتبات المركبة.

INTRODUCTION

In civil engineering construction fields, the merits of materials are based on many factors such as availability, structural strength, durability and workability. It is hardly surprising to know that there is no naturally occurring material "till now" possessed all these properties to a certain desired level, and from this fact, the engineer's efforts foxed on combining more than one material to each other to form a structural member with the aim that only the desirable properties of each material will be utilized by virtue of designated position. Structural member consist of two or more materials is known as "composite member" [1]. In present study, the term composite member refer to the steel beam (section) mantled (fully and partially encased) to reinforced concrete by mechanisms of natural bond (adhesion and friction) with or without the presence of mechanical connector (shear connectors). Encasement of a steel shape increases its stiffness, energy absorption, and drastically reduces the possibility of local buckling of the encased steel. This type of composite member has been used in Japan for more than (4 decades)-(**Wakabayashi 1987**). It also becomes increasingly popular to use the concrete encased steel members in building construction in Taiwan after the **Ji-Ji** earthquake in (1999). A design guide for this type of structural member can be found from the latest edition of the steel reinforced concrete **(SRC)** structures design standards published by **Architectural Institute of Japan** (**AIJ** 2001). Past studies of composite concrete encased steel members have concentrated on the strength and behavior of columns or beam columns **(Procter 1967; Furlong 1968; Naka et al. 1977 Johnson and May 1978; Mirza 1989; Ricles and Paboojian 1994; El-Tawila et al. 1995; Mirza et al. 1996; Munoz and Hsu 1997a, b; El-Tawil and Deievlein 1999**).

Composite Beams Of Concrete Encased Structural Steel Section:

The earliest known form of steel-concrete composite construction, dating from the late (1800s), comprised a steel beam fully or partially encased in concrete, as shown in (Fig. 1). The arrangement was first used in a bridge in **Iowa** and a building in **Pittsburgh**. The encasement provides fire protection but also enhances the bending strength of the steel beam [2].

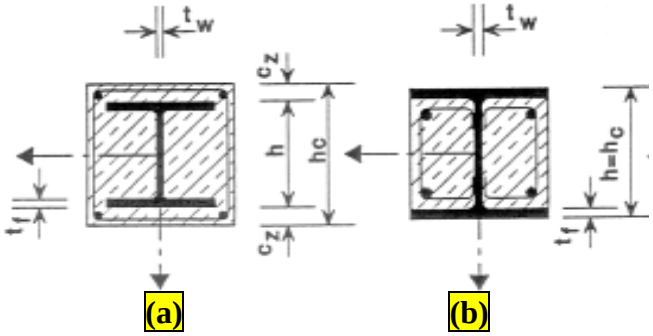

Fig. 1.Composite Beam of Concrete Encased Steel Section [3]:
(a) Fully Encased Composite Beam, (b) Partially Encased Composite Beam.

The local buckling strength also increases in relation to the steel section, and the overall height of both composite beam and composite floor is reduced. In addition, lower construction cost compared to reinforced concrete construction or steel frame system and also shorter construction time can be obtained through the using of encased beams. Therefore, the concrete cast within the flanges of the steel beam is an innovative and interesting alternative that needs to be investigated in details [4]. (Fig. 2). shows different form of composite beam encased (fully or partially) steel section that used nowadays.

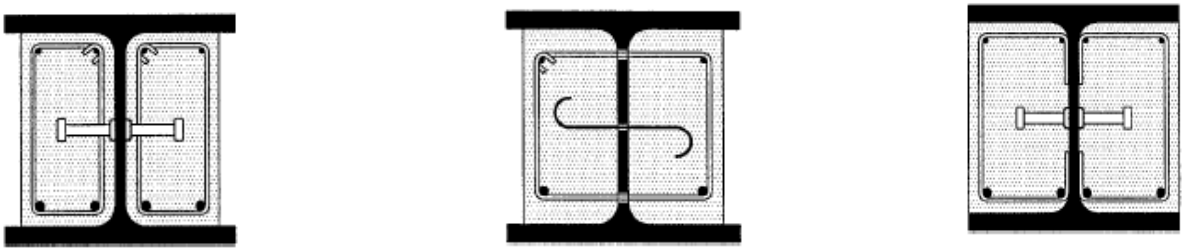

Fig. 2. Different Form of Steel–Concrete Composite Encased Beams [4, 5]: (a) Steel Profile with Studs and Closed Stirrups, (b) Steel Profile with Stirrups through the Web, (c) Steel Profile with Studs and Open Stirrups Welded to the Web.

Preflex Beam:

Preflex beam is a composite beam, which is maximizing the structural advantage of both steel frame and reinforced concrete; it is produced by cambering the steel beam upwards over the span using suitable propping or jacking systems. Preflex beams have been used successfully in a number of road bridges as well as building structures. The typical construction sequence of a precambered beam is as follows [6], see (Fig. 3):

a. In the plant, setup a straight steel I-girder.
b. Prebend the steel girder by applying two concentrated loads at one-third of the span from both sides by using suitable propping or jacking systems.
c. Cast the concrete in form of fully or partially encasement around the steel girder while keeping in place the loads of the prebending phase of the girder.
d. after the hardening of concrete, remove the prebending loads. As a result, the beam goes down, the precamber becomes smaller than the original precamber and the concrete is now subjected to compression [6].

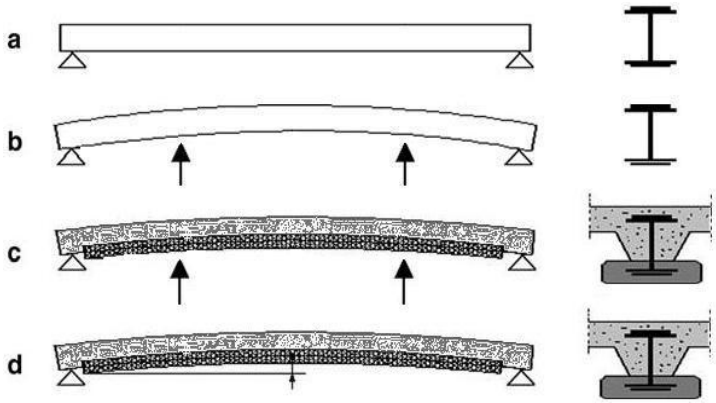

Fig. 3. Schematic Showing Construction Stages of Preflex (precambered) Beam [6].

AVAILABLE EXPERIMENTAL RESEARCH:

Works on encased composite beams dates back to the beginning of the last century, a series of testes have been conducted on this type of composite beam to study the influence of the concrete encasement on the behavior of steel beam section under different loading conditions. In the present study, **Hegger and Goralski, in (2006) [7]**, tested specimens (S1, S2, S3 and S4) are chosen to verify the applicability of **ANSYS** computer program to analyze the encased composite beams and also to investigate the main parameters that affected it's the behavior.

DETAILS OF THE TEST SPECIMENS:

A total of eight simply support (full-scale) laminated composite beams composed of structural steel beam (rolled section) partially encased in high strength concrete were tested under two concentrated loads [7]. Variables of the beams were the studs connecting the encasement with the steel profile. The beams (S1, S3, H1 and H3) were fully shear connected according to (**EURO CODE 1994**); the remaining beams (S2, S4, H2, and H4) contained only one stud above each support for fixing reasons. For the present study the tested specimens (S1, S2, S3, and S4) are chosen. The headed studs of (19 mm) diameter and total post-weld height (125 mm-connect the steel section with the laminated slab) and (120 mm to 80 mm-connect the steel section with the concrete encasement) were directly welded on each side of the web or top flange of the steel section. The aim of studing these experimental beams were to investigate the effectiveness of the high strength concrete encasement (C80/95)-(compression strength equal to 95 N/mm2) under positive and negative bending moment. The cross-sections and loading arrangement for the tested specimens are shown in (Fig. 4), and (Fig. 5). The dimensions of the steel sections, gross-sections and failure mode are given in (Table 1). The material properties are given in (Table 2).

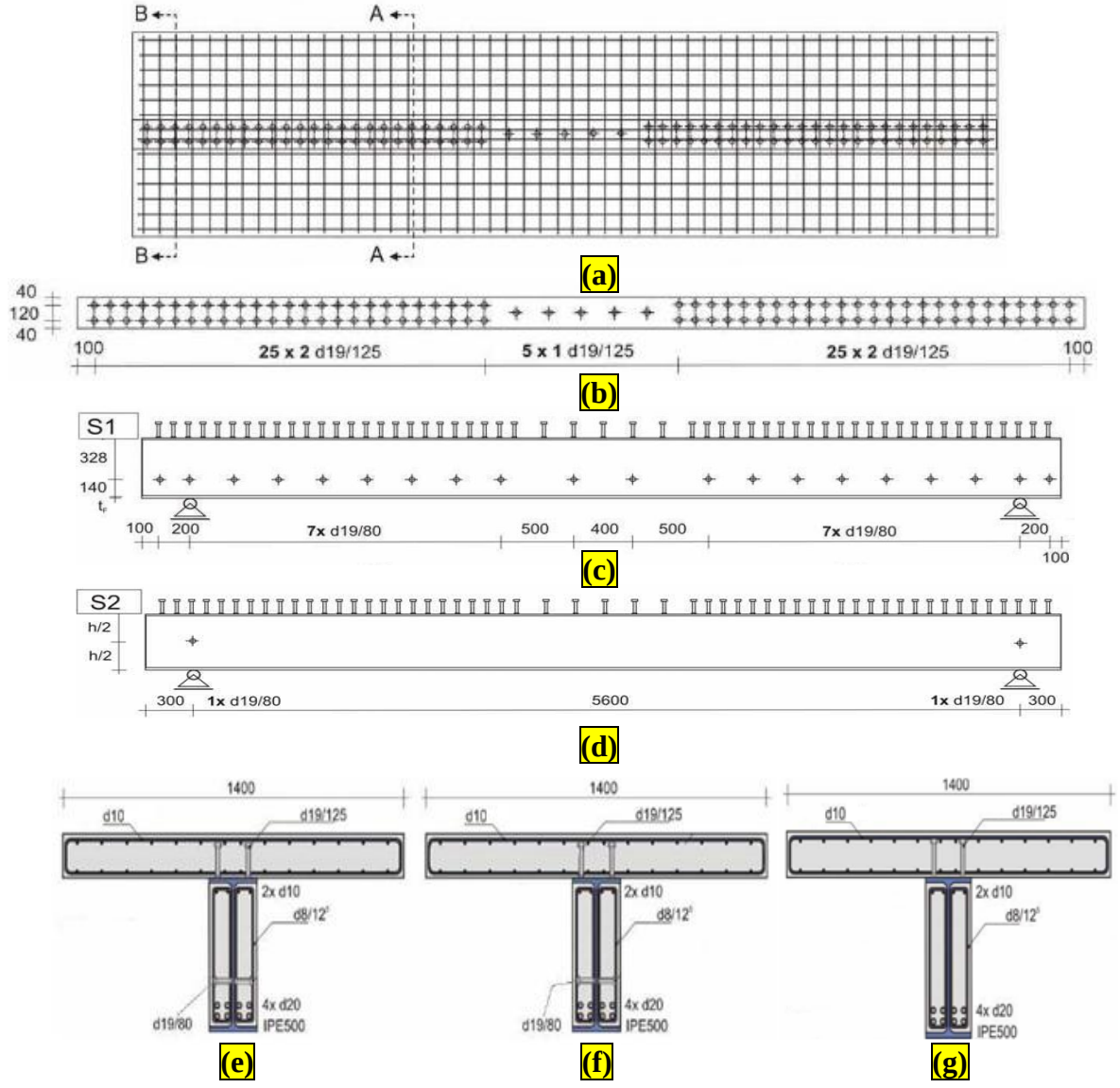

Fig. 4. Geometry of the Laminated Partially Encased Tested Specimens [7]: (a) Flexural and Shear Reinforcement Distributions in the Top Slab (S1+S2), (b) Studs Distribution on the Top Flange (S1+S2), (c) Studs Distribution on the Web (S1), (d) Studs Distribution on the Web (S2), (e) Section (A-A) Specimens (S1+S2), (f) Section (B-B) Specimen (S1), (g) Section (B-B) Specimen (S2), (All dimensions in mm).

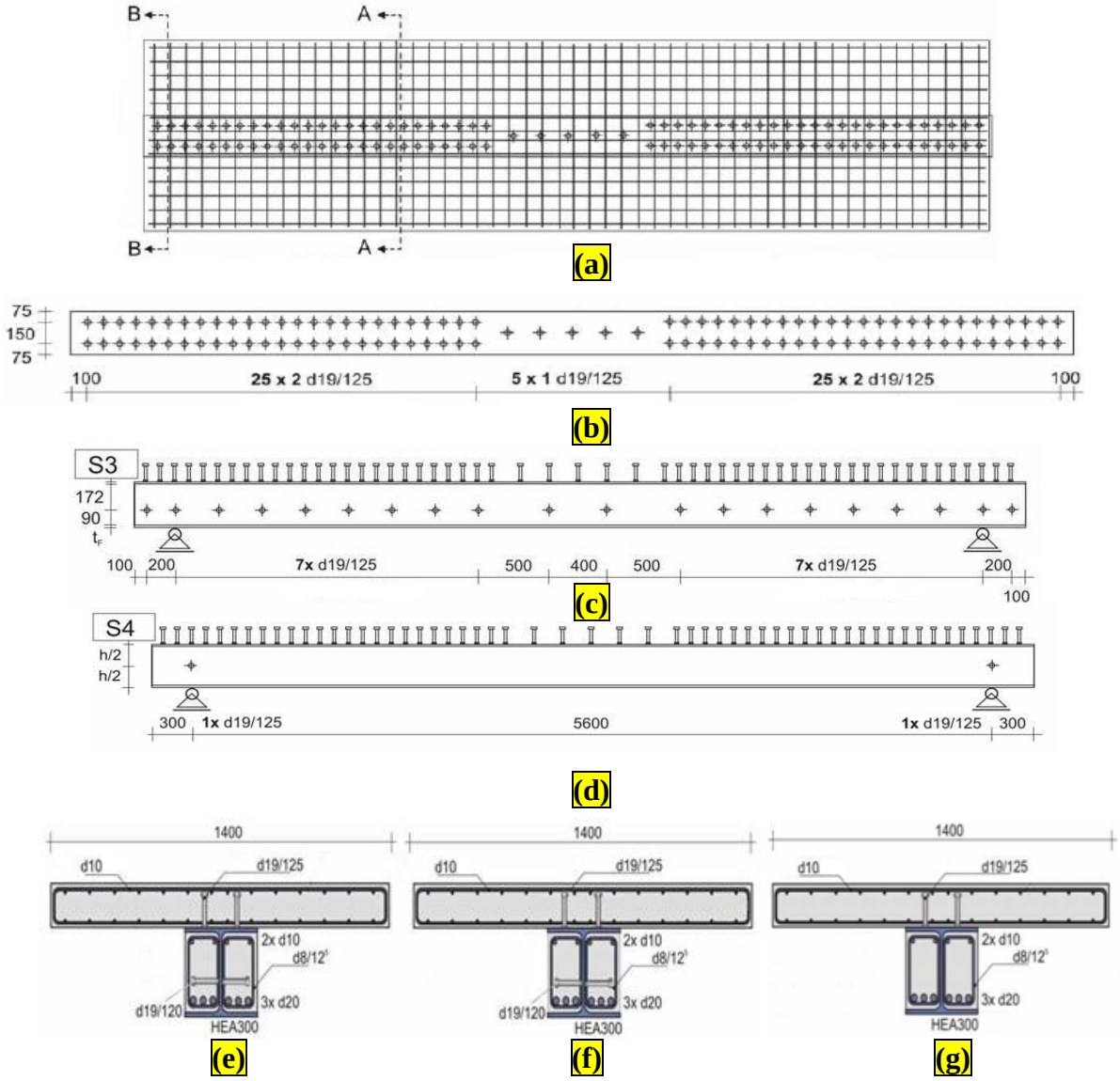

Fig. 5. Geometry of the Laminated Partially Encased Tested Specimens [7]: (a) Flexural and Shear Reinforcement Distributions in the Top Slab (S3+S4), (b) Studs Distribution on the Top Flange (S3+S4), (c) Studs Distribution on the Web (S3), (d) Studs Distribution on the Web (S4), (e) Section (A-A) Specimens (S3+S4), (f) Section (B-B) Specimen (S3), (g) Section (B-B) Specimen (S4), (All dimensions in mm).

Table 1: Descriptions, Dimensions of Steel Sections and Dimensions of Gross-Sections of the Tested Specimens.

Analyzed (Tested) specimen	Steel shape (ds×bf×tw×tf) (mm)	Cross-Section Dimensions(mm)
S1	{500X200X10.2X16}	SLAB(1400X140)
		BEAM(500X200)
S2	{500X200X10.2X16}	SLAB(1400X140)
		BEAM(500X200)
S3	{290X300X8.5X14}	SLAB(1400X140)
		BEAM(290X300)
S4	{290X300X8.5X14}	SLAB(1400X140)
		BEAM(290X300)

Table 2: Material Properties of the Analyzed (Tested) Specimens.

Analyzed (Tested) specimen	S1		S2		S3		S4	
	BEAM	SLAB	BEAM	SLAB	BEAM	SLAB	BEAM	SLAB
Concrete								
Compressive strength-(f'c)-(N/mm2)(♦)	89.000	55.000	83.000	52.000	85.000	53.000	89.000	48.000
Tensile strength-(fcr)-(N/mm2)(♥)	5.860	4.610	5.660	4.480	5.730	4.520	5.860	4.300
Young modulus- (Ec)-(N/mm2)(♣)	44651.0	35100.9	43119.7	34130.1	43636.1	34456.8	44651.0	32791.2
Poisson's ratio-(ν)(♠)	0.2	0.2	0.2	0.2	0.2	0.2	0.2	0.2
Steel section								
Yield stress of steel-(fy)-(N/mm2)(♦)	553		553		504		504	
Ultimate stress of steel-(fy)(N/mm2)(♦)	650		650		528		528	
Young modulus- (Es)-(N/mm2)(♠)	200000	200000	200000	200000	200000	200000	200000	200000
Poisson's ratio-(ν)(♠)	0.3	0.3	0.3	0.3	0.3	0.3	0.3	0.3
Flexural reinforcement	D20 mm D10 mm	D10 mm	D20 mm D10 mm	D10 mm	D20 mm D10 mm	D10 mm	D20 mm D10 mm	D10 mm
Yield stress of steel-(fy)-(N/mm2)(♦)	529 565	565	529 565	565	529 565	565	529 565	565
Ultimate stress of steel-(fy)-(N/mm2)(♦)	659 641	641	659 641	641	659 641	641	659 641	641
Young modulus- (Es)-(N/mm2)(♠)	200000	200000	200000	200000	200000	200000	200000	200000
Poisson's ratio-(ν)(♠)	0.3	0.3	0.3	0.3	0.3	0.3	0.3	0.3
Shear reinforcement (stirrups)	D8 mm	D10 mm	D8 mm	D10 mm	D8 mm	D10 mm	D8 mm	D10 mm
Yield stress of steel-(fy)-(N/mm2)(♦)	619	565	619	565	619	565	619	565
Ultimate stress of steel-(fy)-(N/mm2)(♦)	699	641	699	641	699	641	699	641
Young modulus- (Es)-(N/mm2)(♠)	200000	200000	200000	200000	200000	200000	200000	200000
Poisson's ratio-(ν)(♠)	0.3	0.3	0.3	0.3	0.3	0.3	0.3	0.3
Shear connector (studs)	D19 mm	D19 mm	D19 mm	D19 mm	D19 mm	D19 mm	D19 mm	D19 mm

Yield stress of steel-(fy)-(N/mm2)(♠)	550	550	550	550	550	550	550	550
Young modulus- (Es)-(N/mm2)(♠)	200000	200000	200000	200000	200000	200000	200000	200000
Poisson's ratio-(ν)(♠)	0.3	0.3	0.3	0.3	0.3	0.3	0.3	0.3

Notation	
Symbol	Description
(♣)	Equation (1)
(♠)	Assumed
(♥)	Equation (2)
(♦)	From test

- $E_c = 4733\sqrt{f_c}$ ……..…….…….....….. (1)

- $f_{cr} = 0.622\ \sqrt{f_c}$ ……..……..……..…….. (2)

Where:

E_c = Modulus of elasticity of concrete in (MPa).
f_c= Cylinder uniaxial compressive strength (MPa).
f_{cr}= tensile strength of concrete (MPa).

FINITE ELEMENT MODEL:

SOFTWARE, ELEMENT TYPES AND MESH CONSTRUCTION:

Advances in computational features and software have brought the finite element method within reach of both academic research and engineers in practice by means of general-purpose nonlinear finite element analysis packages, with one of the most used nowadays being **ANSYS**. The program offers a wide range of options regarding element types, material behaviors and numerical solution controls, as well as graphic user interfaces (known as GUIs), auto-meshers [8], and sophisticated postprocessors and graphics to speed the analyses. In the present study, the structural system modeling is based on the use of this commercial software. The finite element types considered in the model are as follows: elastic-plastic shell **(SHELL43)** and solid **(SOLID65)** elements for the steel section and the concrete slab, respectively, and nonlinear springs **(COMBIN39)** to represent the shear connectors. Both longitudinal and transverse reinforcing bars are modeled as discrete using **(LINK8)** element. Rigid-to-flexible contact mechanisms are used to model the interface contact surface between the structural steel section and the encased concrete. The rigid target surface (encased steel section which is represented by **(SHELL43)** element) modeled with **(TARGE170)** elements, while the contact flexible surface (concrete encasement which is represented by **(SOLID65)** elements) modeled with **(CONTA173)** elements. The element **(SHELL43)** is defined by four nodes having six degrees of freedom at each node. The deformation shapes are linear in both in-plane directions. The element allows for plasticity, creep, stress stiffening, large deflections, and large strain capabilities [8]. The element **(SOLID65)** is used for three dimensional modeling of solids with or without reinforcing bars (rebars capability). The element has eight nodes and three degrees of freedom (translations) at each node. The concrete is capable of cracking (in three orthogonal directions), crushing, plastic deformation, and creep [8]. The rebars **(LINK8)** element are capable of sustaining tension and compression forces, but not shear, being also capable of plastic deformation and creep and have two nodes with three translation degrees of freedom at each node. The element **(COMBIN39)** is defined by two node points and a generalized force–deflection curve and has longitudinal or torsional capability. The longitudinal

option is a uniaxial tension–compression element with up to three degrees of freedom (translations) at each node. A typical finite element mesh for a composite encased beam is shown in (Fig. 6).

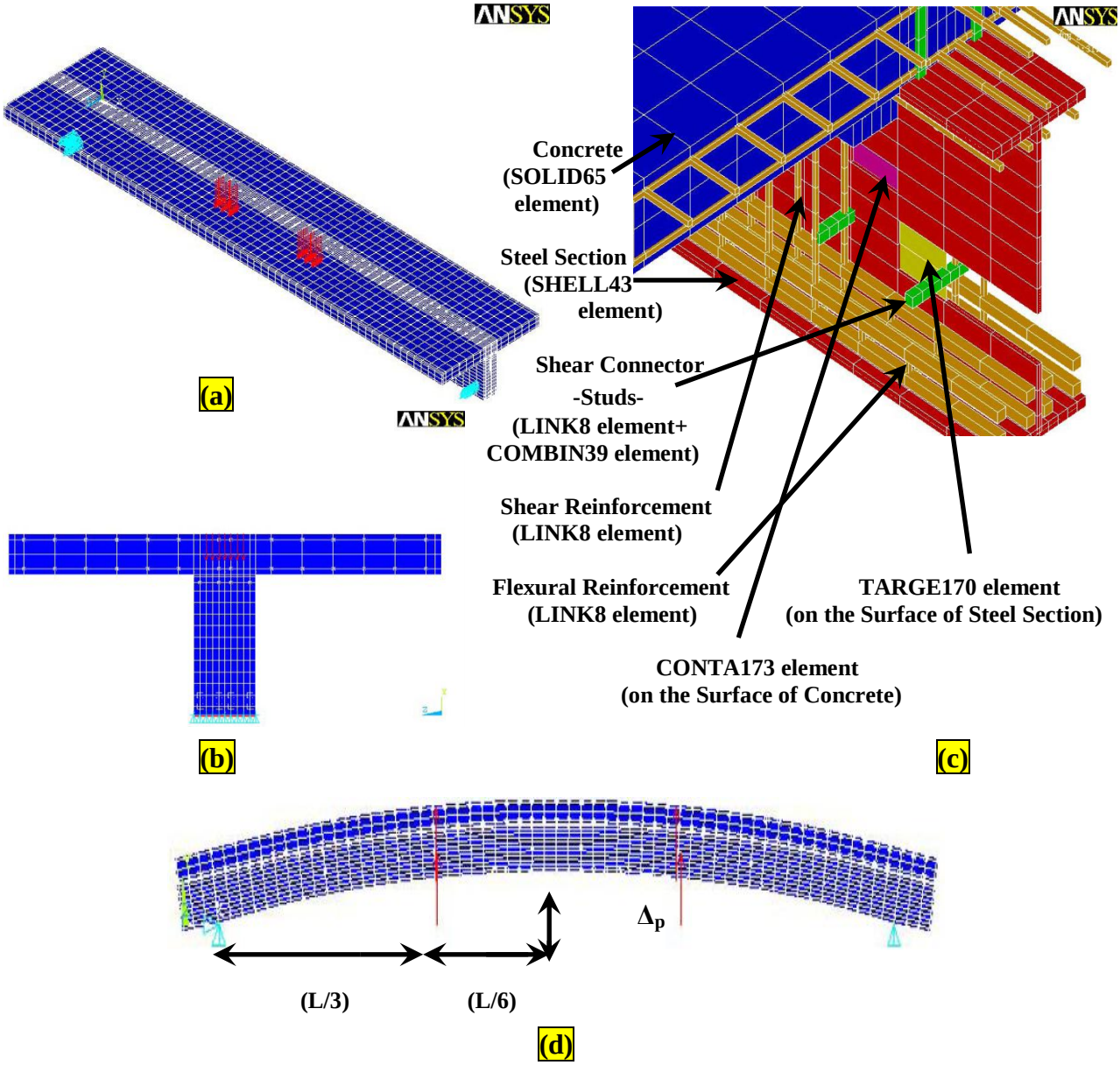

Fig. 6. Finite Element Mesh for (S1) Model:
(a) Isometric-View, (b) Front-View, (c) Internal Section, (d) Preflexing Shape.

The following equations are used to calculate the amount of forces required to produce the upward movement (cambering) of simply support steel section subjected into two forces at distance (L/3) from its two ends for a given allowable compressive stress in the steel beam [9].

Upward deflection $\Delta_p = \frac{23PL^3}{648EI}$ ..... (3)

Bending moment $M = \frac{PL}{3}$ ..... (4)

Compression flange stress $\sigma = \frac{My}{I}$ ..... (5)

By substituting in equation (3):

$$\Delta_p = \frac{23\sigma L^2}{216Ey} \quad \text{..... (6)}$$

$$P = \frac{3\sigma I}{Ly} \quad \text{..... (7)}$$

Where:

Δ_p in **(mm)**= cambering produced in the steel section.

P= force applied to the a steel section to produced cambering.

σ= Allowable compressive stress in the steel beam - (N/mm2) are given in (Table 2).

L= Clear span of the tested specimens-(mm).

E=Es= (Young modulus of steel=200,000 N/mm2).

y= Distance from the steel section centroid to the top surface of compression flange in (mm).

MATERIAL MODELIND:

The von Mises yield criterion with isotropic hardening rule (multilinear work-hardening material) is used to represent the steel beam (flanges and web) behavior. The stress–strain relationship is linear elastic up to yielding, perfectly plastic between the elastic limit and the beginning of strain hardening. The von Mises yield criterion with isotropic hardening rule is also used for the reinforcing steel. An elastic-linear-work hardening material is considered, with tangent modulus being equal to (1/10000) of the elastic modulus, in order to avoid numerical problems. The values measured in the experimental tests for the material properties of the steel components (steel beam and reinforcing bars) are used in the finite element analyses. The concrete encasement behavior is modeled by a multilinear isotropic hardening relationship, using the von Mises yield criterion coupled with an isotropic work hardening assumption. The uniaxial behavior is described by a piece-wise linear total stress–total strain curve, starting at the origin, with positive stress and strain values, considering the concrete compressive strength ($\acute{f}_c$) corresponding to a compressive strain of (0.2%). The stress–strain curve also assumes a total increase of (0.05 N/mm2) in the compressive strength up to the concrete strain of (0.35%) to avoid numerical problems due to an unrestricted yielding flow. The concrete element shear transfer coefficients considered are: (0.25) for open crack and (0.8) for closed crack. Typical values range from (0 to 1), where (0) represents a smooth crack (complete loss of shear transfer) and (1) a rough crack (no loss of shear transfer). The default value of (0.6) is used as the stress relaxation coefficient (a device that helps accelerate convergence when cracking is imminent). The crushing capability of the concrete element is also disabled to improve convergence. The concrete encasement compressive strength is taken as the actual cylinder strength test value. The concrete tensile strength and the Poisson's ratio are assumed as (1/10) of its compressive strength and (0.2), respectively. The concrete elastic modulus is evaluated according to equation (1) mentioned above. The model allows for any pattern of stud distribution to be considered. In all analyses, the number/spacing of studs adopted in the experimental programmers is utilized. As far as the shear connector behavior is concerned, the load–slip curves for the studs are used (obtained from available push-out tests) by defining a table of force values and relative displacements (slip) as input data for the nonlinear springs. These springs are modeled at the steel–concrete interface [10], as shown in (Fig. 7). the behavior of the interface surface of contact between the steel section and concrete encasement is modeled according to the basic **Coulomb friction model**, in which, two contacting surfaces can carry shear stresses up to a certain magnitude across their interface before they start sliding relative to each other. This state is known as sticking. The **Coulomb friction model** defines an equivalent shear stress (τ), at which sliding on the surface begins as a fraction of the contact pressure (p) as [8]:

$$\tau_{lim} = \mu p + COHE, \quad |\tau| \le \tau_{lim} \quad \text{..... (8)}$$

where:

τ_{lim} = limit shear stress, τ= equivalent shear stress, μ= the friction coefficient, P= constant normal pressure, COHE= cohesion sliding resistance (stress unite).

Once the shear stress is exceeded, the two surfaces will slide relative to each other. This state is known as sliding. The sticking/sliding calculations determine when a point transitions from sticking to sliding, see (Fig. 8). **ANSYS** provides two models for Coulomb friction [8]: Isotropic friction (2-D and 3-D contact): which is based on a single coefficient of friction (MU) and the orthotropic friction (3-D contact): which is based on two coefficients of friction (MU1 and MU2). In the present study, (3-D) Isotropic friction model is used with single coefficient of friction (MU), and the cohesion sliding resistance (COHE) set to (0.00) making (Fig. 9(a)) change to (Fig. 9(b)).

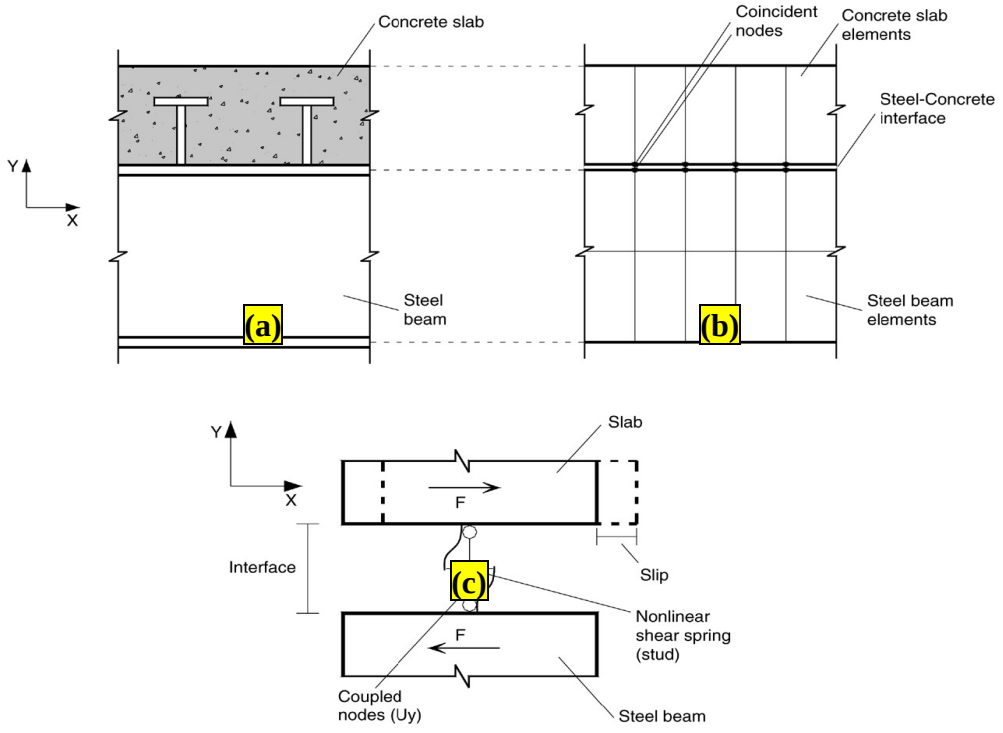

Fig. 7. Modeling of shear connectors (longitudinal view) [10]:

(a) Shear studs in a typical composite beam. (b) Shear studs in a typical composite beam finite element mesh. (c) Representation of the shear stud model.

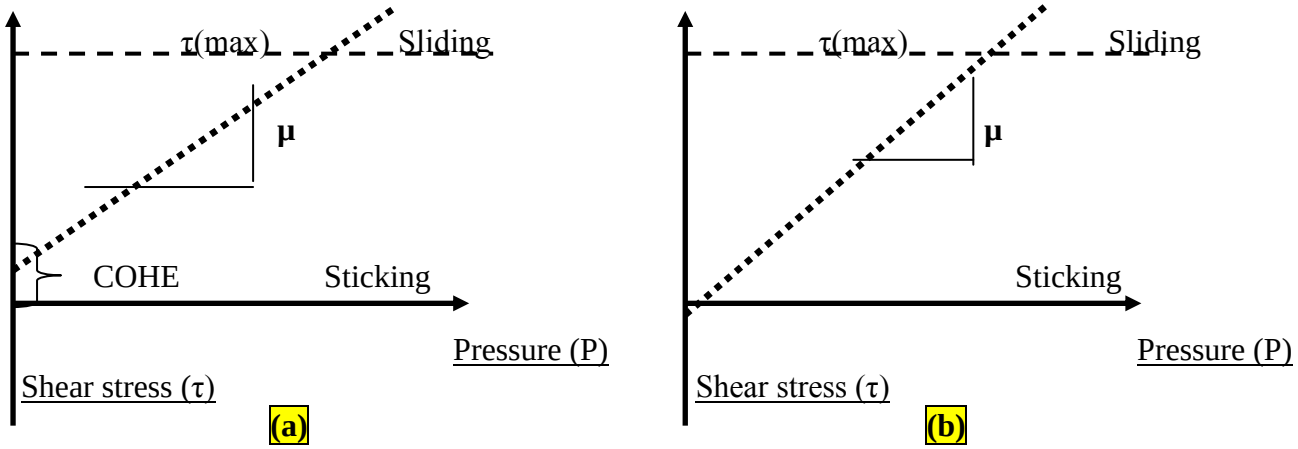

Fig. 8. Frictional Models [8].

APPLICATION OF THE LOAD AND NUMERICAL CONTROL:

Regarding application of the load, concentrated loads are incrementally applied to the model by means of an equivalent displacement to overcome convergence problems (displacement control). For the convergence criterion, the **L2-Norm** (square root sum of the squares) of displacements is considered. Concentrated loads are represented by means of point loads applied at nodes. These concentrated loads are also applied to the model incrementally using the load control strategy and the **L2-Norm**. The tolerance associated with this convergence criterion (**CNVTOL** command of **ANSYS**) and the load step increments are varied in order to solve potential numerical problems. Whenever the solution does not converge for the set of parameters considered, as far as load step size and converge criterion are concerned, the **RESTART** command is used in conjunction with the **CNVTOL** option [1]. **ANSYS** allows two different types of restart: the single-frame restart and the multi-frame restart, which can be used for static or full transient structural analyses. The single-frame restart only allows the user to resume a job at the point it stopped. The multi-frame restart can resume a job at any point in the analysis for which information is saved. This capability enables multiple model analyses, presenting more options for data retrieval after an undesired aborted solution. The second approach is used throughout the present analyses. For the case in which only one point load is applied to the system, there is a direct relationship between force and displacement, making the displacement control method easier to be utilized. The load control method is, however, less efficient than the displacement control method in nonlinear analyses. This fact is observed especially when the applied load approaches the ultimate load of the system, as an incremental increase in the load leads to a significant increase in the corresponding displacements, causing difficulties in terms of numerical convergence. For the type and size of the finite element problem investigated, the load control method demanded, on average, (70%) more disk space and took (150%) longer to be processed than similar displacement control solutions. The finite element analysis of the models was set up to examine two main behaviors: (initial cracking of the composite encased beams and the strength limit state). The Full Newton-Raphson method of analysis is used to compute the nonlinear response. The application of the loads up to failure was done incrementally as required by the Newton-Raphson procedure [1].

ANALYSIS PROCESS FOR THE ANALYZED FINITE ELEMENT MODELS:

ANALYSIS OF THE STRAIGHT ENCASED COMPOSITE BEAMS:

The finite element analyses for the straight simply support composite encased beams under concentrated forces have been carried out using static analysis type. The solution controls command dictates the use of a linear or non-linear solution for the finite element model. The program behavior upon non-convergence for this analysis was set such that the program will terminate but not exit. The most important typical commands utilized in a nonlinear static analysis are shown in Table (3). The rest of the commands were set to defaults.

Table 3: The Most Important Commands Used to Control Nonlinear Analysis.

Commands	Description
solution printout controls	all solution items such as {nodal DOF solution, nodal reaction loads, element solution (element nodal stresses+element elastic and plastic strains…etc),…etc}
print frequency	write every substep
controls for database and results file written.	all solution items such as {nodal DOF solution, nodal reaction loads, element solution (Element nodal stresses+element elastic and plastic strains…etc),…etc}
print frequency	write every substep

time at end of loadstep	**(experimental failure load)X(1.1)**
time Step size	**(1%) from the time at end of loadstep**
automatic time stepping	**on**
max no. of substeps	**time Step size**
min no. of substeps	**(10%) from the max no. of substeps**

At first trials for the analysis, the values for the convergence criteria (force and displacement) are set to defaults except for the tolerances. The tolerances for force and displacement are set as (15 times) the default values. However, when the composite encased beams began cracking, convergence for the non-linear analysis was impossible with the default values. The displacements converged, but the forces did not. Therefore, the convergence criterion for force was dropped and the reference value for the Displacement criteria was changed to (5), this value is then multiplied by the tolerance value of (0.01) to produce a criterion of (0.05) during the nonlinear solution for convergence. A small criterion must be used to capture correct response. Table (4) represents the commands used for the nonlinear algorithm and convergence criteria.

Table 4: Nonlinear Algorithm and Convergence Criteria Parameters.

Commands	**Description**	
equilibrium iteration	**100**	
criteria to stop an analysis	**stop and stay**	
Set Convergence Criteria		
Label	F (force)	U (displacements)
reference value	**calculated**	**calculated**
convergence tolerance	**0.001**	**0.010**
Norm	**L2 (SRSS value)**	**L2(SRSS value)**
Minimum reference value	**Default**	**Default**

ANALYSIS OF THE PREFLEX ENCASED COMPOSITE BEAMS:

Analyses for the preflex encased composite beams were similar to the analyses of the straight encased composite beams. However, different load steps were used. The first load step taken was to produce camber in the steel beam only in which the upward movement of the beam resulted, meanwhile all others element consisting the encased beams except the shear connector element **(COMBIN39** element) considered to be a **(DEAD ELEMENTS)** according to **(ELEMENT BIRTH AND DEATH OPTION)** supported by **ANSYS** commands. **RESTART** command then used to re-analyze the beams due to its original state of loading (Experimental Researches papers), during this, the flexural reinforcement, shear reinforcement and concrete element are re-activated **(BIRTH**) and the two preflexing forces are neutralized by two forces having the same magnitude but opposite direction. The preflexing loads are removed. As a result, the beam goes down a little due to self weight (**gravity-loads**) and the stress recovery of the steel beam, the precamber amount becomes smaller than the original cambering, and the concrete is now subjected to compression. The moment-rotation curves for analyzed laminated composite partially encased beams {{(S1+S2+S3+S4) **Hegger** and **Goralski**, (2006) [7]}} which were obtained numerically by the finite element method using **ANSYS (V.10)** computer program for straight and preflex steel section are compared with the experimental results and presented in (Fig. 10) through (Fig. 13); respectively. The goal of the

comparison of the finite element models and the beams experimental works is to ensure that the elements types, meshing, material properties, real constants and convergence criteria are adequate to model the response of the beams. The angle of rotation (φ_s)-(which is idealized the X-axis of the moment-rotation curves for the analyzed specimens (S1, S2, S3 and S4) is obtained by the secant angle of the displacement at mid span and represent the rotation of cross-section of the laminated partially encased composite beams at mid span [7]. see (Fig. 9).

φ_s= Secant Angle = **ARCTAN (Δ/0.5L)** ..... (9)

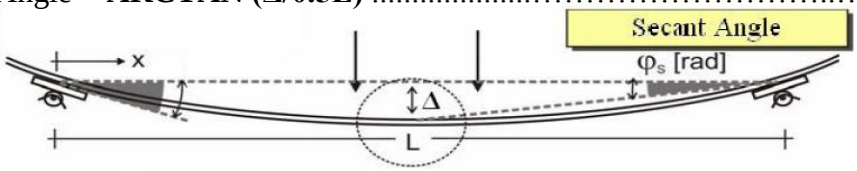

Fig. 9. Definition of the Secant Angle (φ_s) [7].

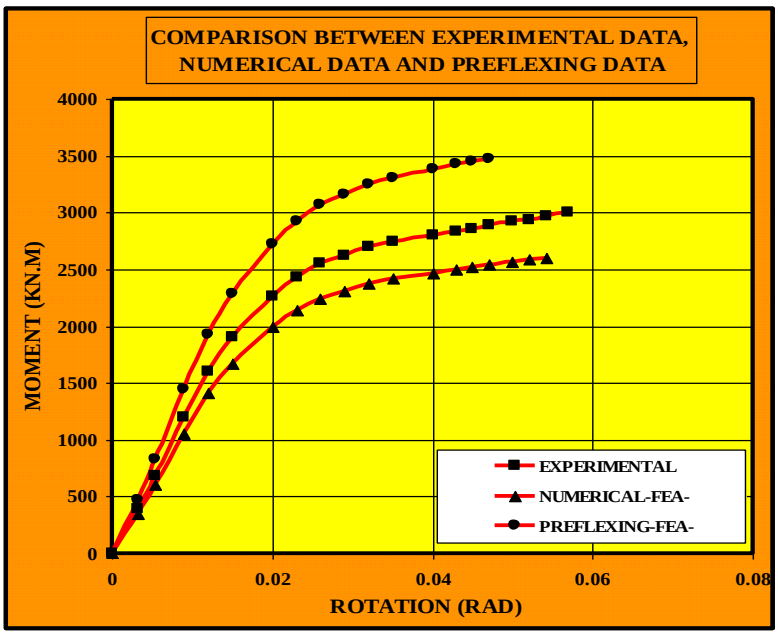

Fig. 10. Finite Element Analysis Result for Model (S1).

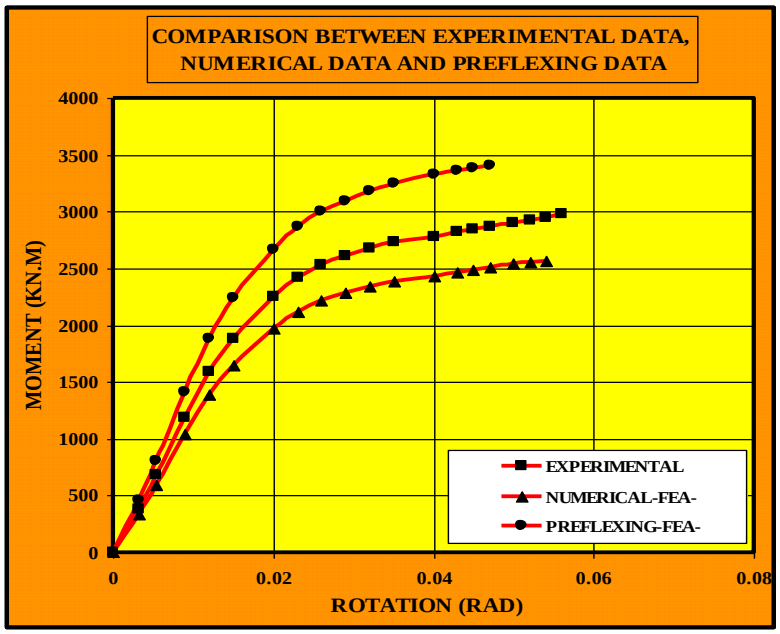

Fig. 11. Finite Element Analysis Result for Model (S2).

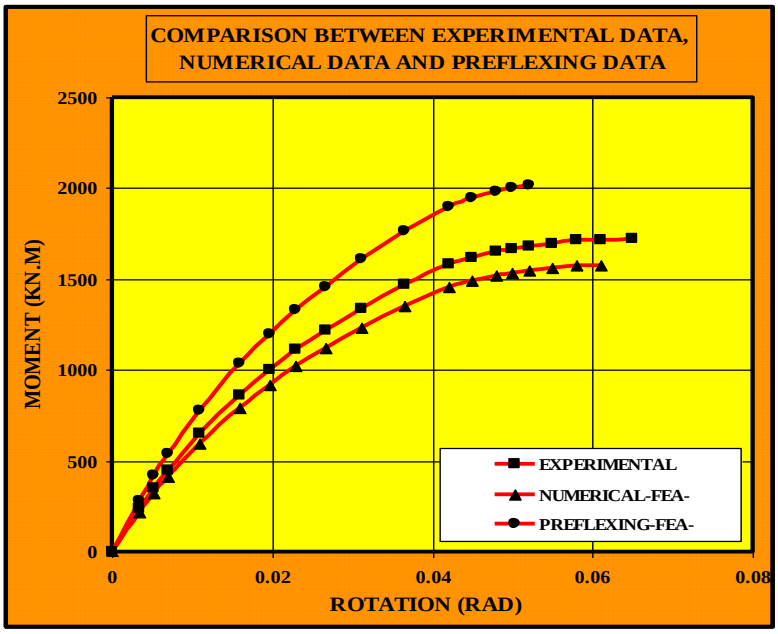

Fig. 12. Finite Element Analysis Result for Model (S3).

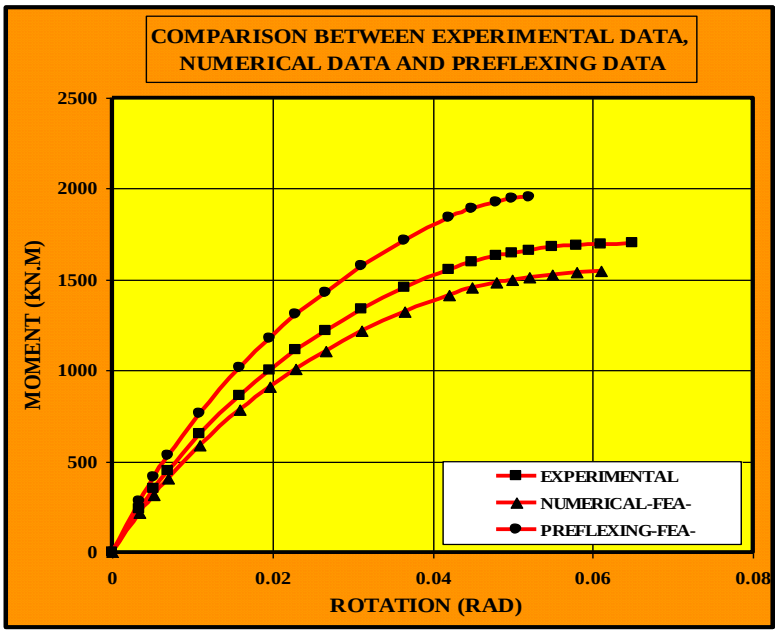

Fig. 13. Finite Element Analysis Result for Model (S4).

BEHAVIOR AT ULTIMATE MOMENTS:

The analytical and experimental values of the maximum moments for straight and preflex composite encased beams which presented in (Fig. 10) through (Fig. 13); respectively, are summarized in (Table 5). Table 5 showed that the preflexed moment of models (S1+S3)-(fully shear connection specimens) are higher than the models (S2+S4)-(partially shear connection specimens) this is due to the numerous presence of shear studs in models (S1+S3), were the longitudinal shear force occurred mainly by friction forces acting at the interface among the concrete encasement and the structural steel are well transfer by shear studs, and also the confinement effect of the steel profile in some areas of the concrete increases the preflexing capacity of the encased beams. The analyses

finished (Done) for the laminated partially encased composite analyzed specimens (S1+S2+S3+S4) due to the crushing of concrete in the compression zone.

Table 5: Comparison between Analytical and Experimental Values of the Ultimate Moments.

Tested specimen	Experimental (maximum moments)	Analytical (maximum moments)-straight beams	A%	Analytical (maximum moments)-preflex beams	B%
S1	3001	2595	13.5	3473.78	13.6
S2	2981	2564	14	3408.89	12.5
S3	1723	1578	8.4	2014.6	14.4
S4	1703	1544	9.3	1955.8	13
Notation					
Symbol	Description				
A%	$\frac{(M_u)_{exp} - (M_u)_{ANSYS\text{-}Straight}}{(M_u)_{exp}}$				
B%	$\frac{(M_u)_{ANSYS\text{-}Preflex} - (M_u)_{exp}}{(M_u)_{ANSYS\text{-}Preflex}}$				

BEHAVIOR AT MAXIMUM ROTATIONS:

The analytical and experimental values of the maximum rotations for straight and preflex composite encased beams are summarized in (Table 6). The moment rotations curves which presented in (Fig. 10) through (Fig. 13); respectively, for the analyzed specimens in which the corresponding experimental, theoretical and preflexing curves are superimposed, show that the curves are lie very close to each other at initial stages for all the specimens. However, there seems to be some deviation between the results near the failure. The discrepancy may be due to the inadequacy in concrete and interface behavior modeling. It was found that the rotations are nearly (85% to 95%) the rotations of the same experimental beam for straight beam situation, and (65% to 80%) of the same experimental beam for preflexed beam situation.

Table 6: Comparison between Analytical and Experimental Values of the Maximum Rotations.

Tested specimen	Experimental Rotations	Analytical (Rotations) straight beams	Analytical (Rotations) preflex beams
S1	0.057	0.054	0.046
S2	0.057	0.055	0.048
S3	0.065	0.061	0.05
S4	0.066	0.062	0.052

THE PARAMETRIC STUDY:

A parametric study has been done on the same samples that have been analyzed. Many parameters can be studied to examine the effect of each parameter on the behavior of the models results. Some models were chosen to study the effect of encased concrete in the increasing of moment-bearing capacity, meanwhile other are chosen to study the slip along the composite partially

encased beams length. The strain distributions along the steel section and encased concrete depth are also examined. The Poisson's ratio of concrete and the effect of cambering of steel-section are also investigated.

EFFECT OF THE ENCASED CONCRETE IN THE INCREASING OF THE LOAD-CARRYING CAPACITY:

The partially laminated encased beams (S1) and (S3), which were described in details in (Fig. 4) and (Fig. 5), are chosen to examine the influence of the encased concrete in the steel-section on the moment-rotation capacity behavior. It is observed that the moment- rotation capacity for the composite beams (S1) and (S3) are reduced by (28.3%) and (27.4%) respectively, with the absence of the encased concrete as shown in Fig. (14) and Fig. (14) respectively. It should be mentioned that the analyses made for the composite beams (S1) and (S3) in the presence of the laminated slab and shear studs distribution on the top flange of the steel section but without encased concrete in the steel-section.

Fig. (14) and Fig. (15) respectively, shows that the moment- rotation capacity for the composite beams are reduced by (57.6%) and (63.5%) for the beams (S1) and (S3) respectively with the absence of the encased concrete and the laminated reinforced slab (steel section only).

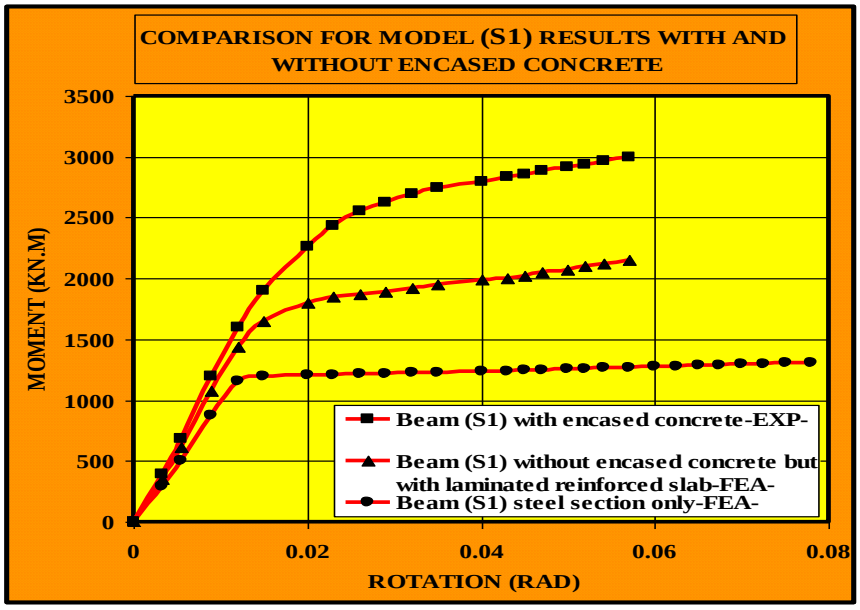

Fig. 14. Finite Element Results of Model (S1) with and without the Encased Concrete in the Steel Section.

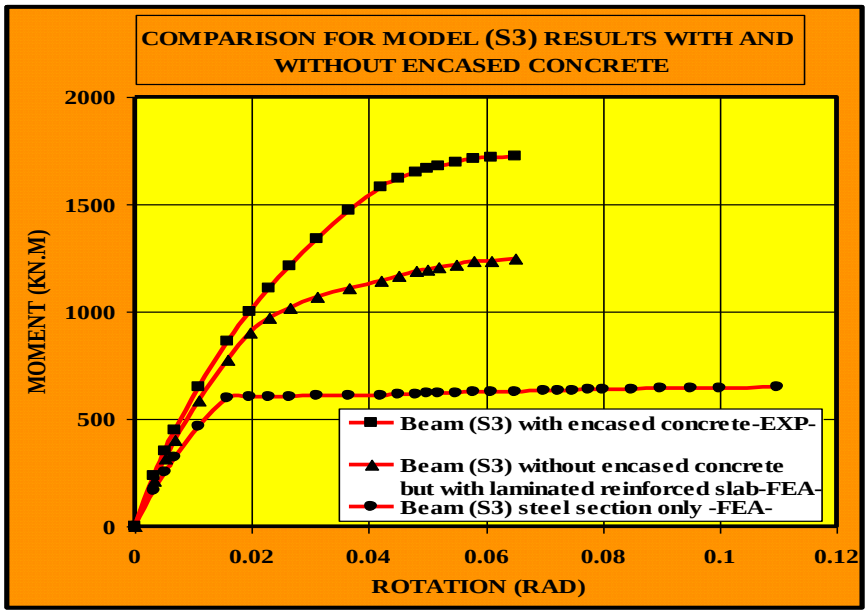

Fig. 15. Finite Element Results of Model (S3) with and without Encased Concrete in the Steel Section.

THE EVALUATION OF SLIPS ALONG THE COMPOSITE ENCASED BEAMS INTERFACE:

The partially laminated encased beams (S1), (S2), (S3) and (S4) which were described in (Fig. 4) and (Fig. 5) are chosen for the evaluation of the slip along the steel-encased concrete interface surface length under different loading magnitudes (0.5 Mu and 0.85 Mu). It is observed that the value of slips near the point of load application is more than the other values along the steel-encased concrete interface surface.

It is also observed that the values of slips for the composite encased beams (S1) and (S3) are less than (S2) and (S4) due to the presence of shear studs (full shear connections) as shown in Fig. (16) and Fig. (17) respectively. It should be mentioned that the values of the slips were obtained from the (DOF solution, X-component of displacement).

Note:- the slips behavior along the beams length take a nonlinear configuration, but in Fig. (16) and Fig. (17) respectively, are drawing linearly for simplifying reasons.

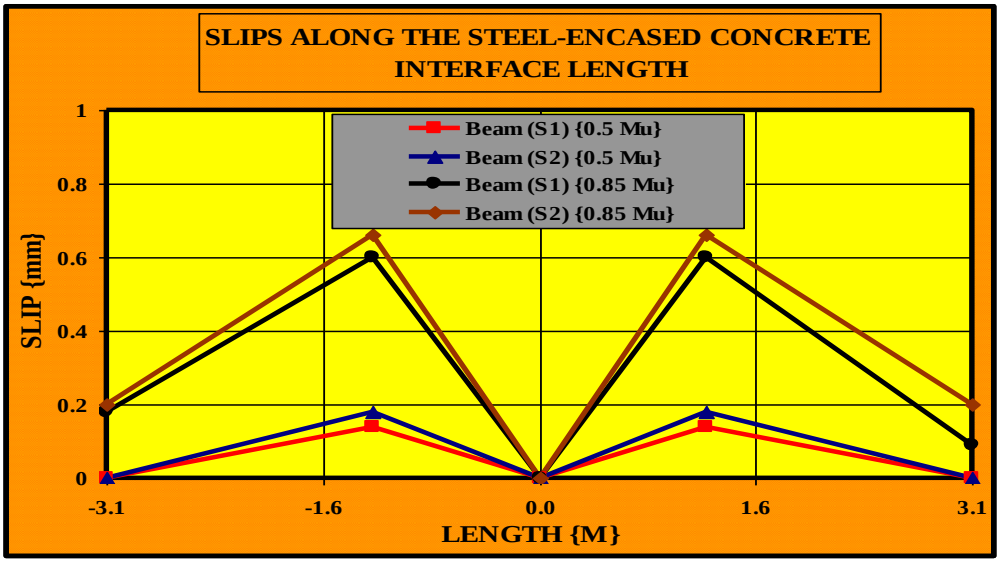

Fig. 16. Finite Element Results of Model (S1 and S2) to Show the Slips along the Steel-Encased Concrete Interface.

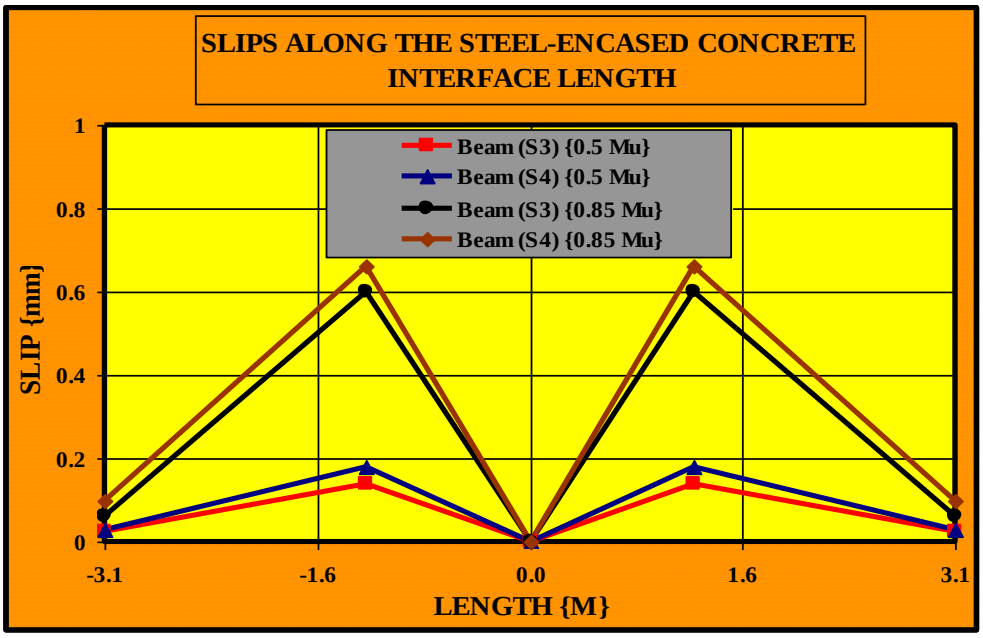

Fig. 17. Finite Element Results of Model (S3 and S4) to Show the Slips along the Steel-Encased Concrete Interface.

THE EVALUATION OF STRAIN DISTRIBUTIONS ALONG THE STEEL SECTION AND ENCASED CONCRETE DEPTH:

The partially laminated encased beams (S1) and (S2) which were described in details in (Fig. 4) are chosen to examine the strain distributions along the depth of both steel section and concrete encasement under different loading magnitudes as shown in (Fig. 18) through (Fig. 21).

It is observed that the values of strains at the steel-encased concrete surface (contact plane) for the model (S1) are nearly the same due to the fully shear connection of this model in comparative with the model (S2) were the strains values at the contact plane between the steel section and concrete encasement showing miner diverging due to the partially shear connection, see (Fig. 22).

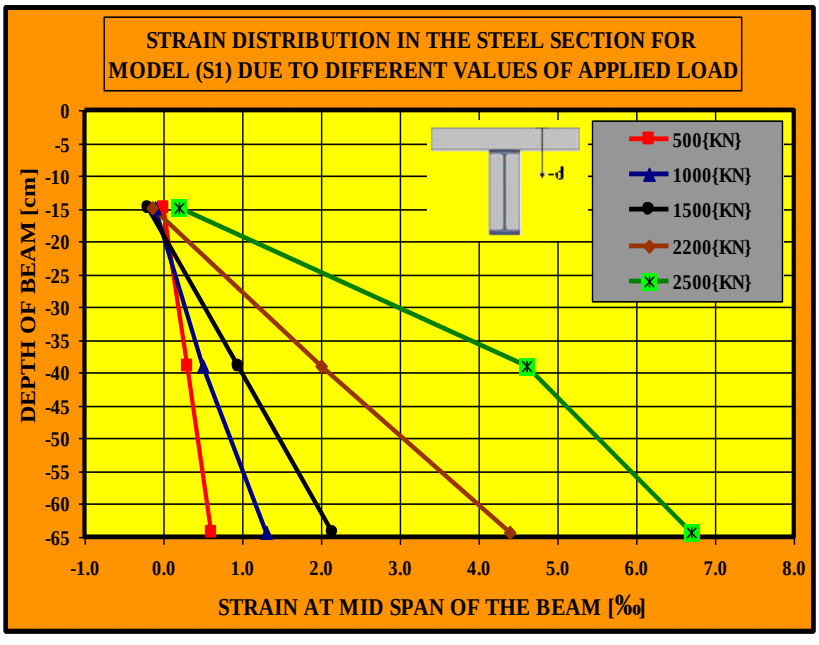

Fig. 18. Strain Distribution along the Depth of Steel Section for Model (S1).

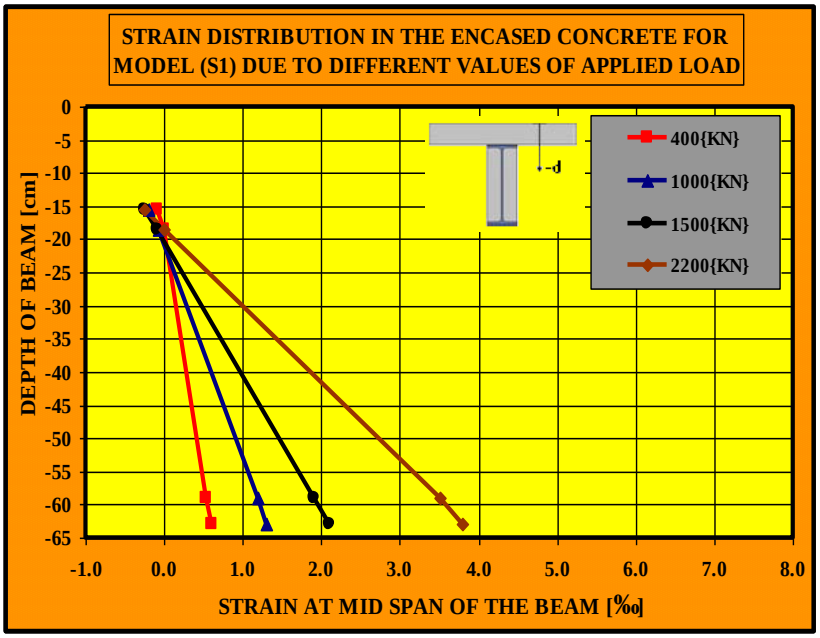

Fig. 19. Strain Distribution along the Depth of Concrete Encasement for Model (S1).

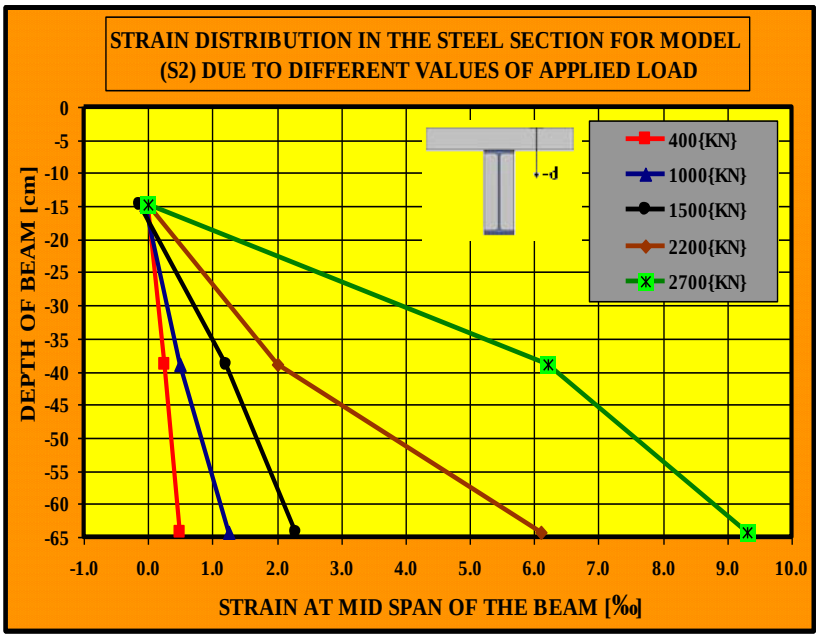

Fig. 20. Strain Distribution along the Depth of Steel Section for Model (S2).

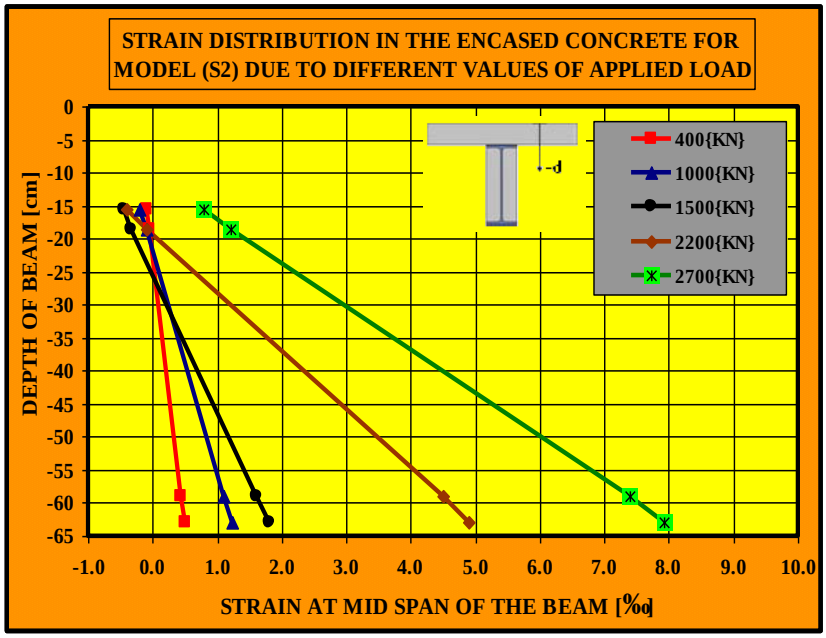

Fig. 21. Strain Distribution along the Depth of Concrete Encasement for Model (S2).

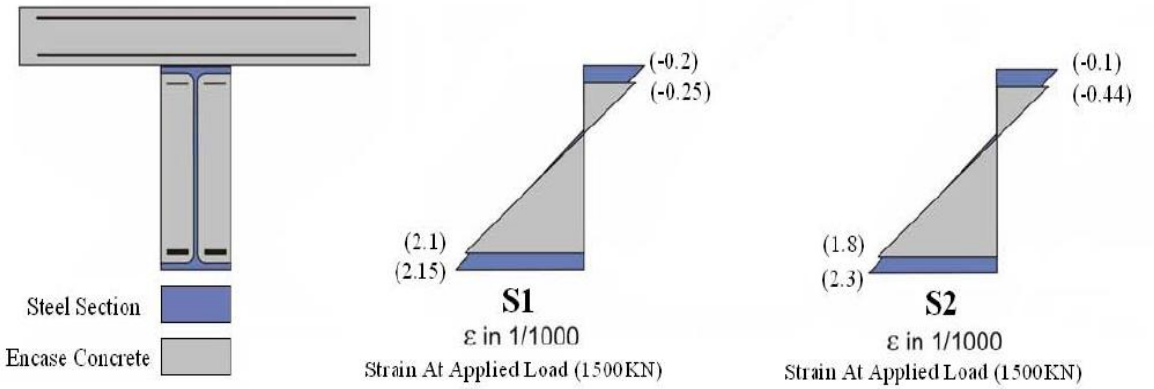

Fig. 22. Strain Difference between Models (S1) and (S2) along the Depth of Concrete Encasement and Steel Section.

Effect Of Concrete Poisson's Ratio On The Behavior Of Model (S3):

The composite encased beam (S3) has been chosen to study the effect of variation of the concrete Poisson's Ratio on its behavior. This beam is described in details in (Fig. 5). The beam has an assumed concrete Poisson's Ratio equal to (ν=0.2**)** and it has been reanalyzed for values of (0.17 and 0.15). As shown in (Fig. 23). the ultimate load capacity of this beam has also insignificant effect with reduction of Poisson's ratio value, and the ratio of reduction in the ultimate load capacity is (2.5% and 4%) for the concrete Poisson's ratio values (0.17 and 0.15) respectively.

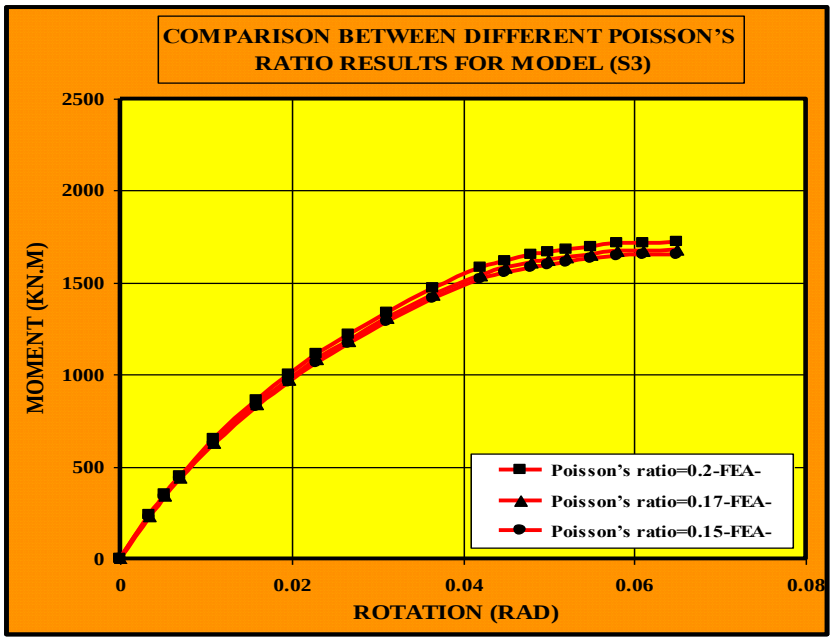

Fig. 23. Effect of Poisson's Ratio on the Behavior of Model (S3).

Effect Of Cambering Of Steel Section For The Model (S4):

The composite laminated partially encased beam (S4) has been chosen to study the effect of cambering of the I-steel section on its behavior. This beam is described in details in (Fig. 5). When the model is preflexed for a given allowable compressive stress in the steel equal to its yield stress (504 N/mm2), the predicted ultimate load of this beam is increased by (13%) due to an amount of upward deflection (57.989 mm) obtained by Equation (6). When the beam is reanalyzed using (250 N/mm2) for the yield stress of steel, the predicted ultimate load of this beam is increased by (6.1%) due to preflex deflection (28.78 mm), as shown in (Fig. 24).

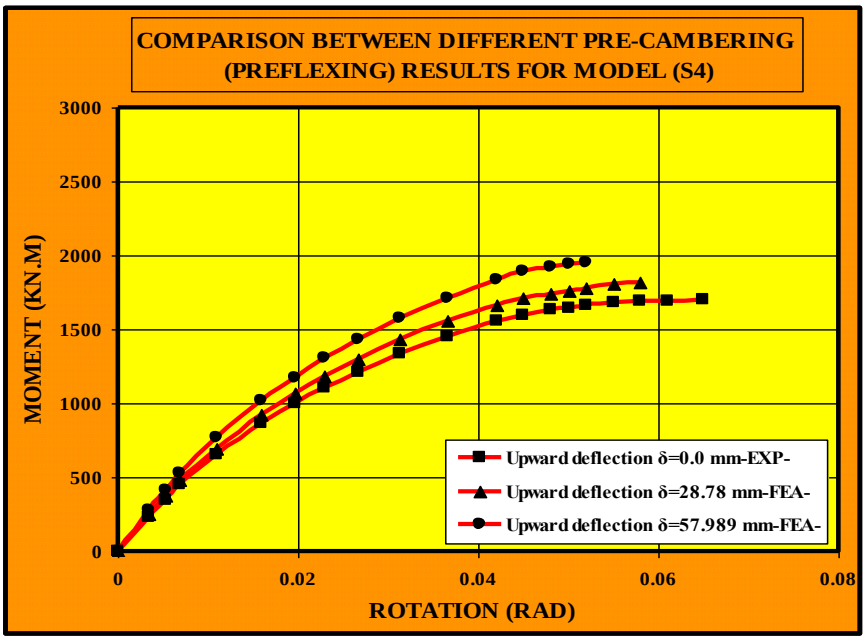

Fig. 24. Effect of Cambering of Steel Section on the Behavior of Beam (S4).

CONCLUSIONS:

Based on the results of this investigation, the following conclusions can be drawn:

- The modeling of the investigated beams by the finite element method gives results which are close to the experimental results for the analysis of composite encased beams consisting of preflex steel section.
- The failure load given by **ANSYS** computer program are close to that measured during experimental test.
- Preflexing of the steel I-beam by introducing initial cambering enhances the strength in comparison with the same simply supported composite beam consisting of steel section encased into concrete without preflexing by relatively (15%) and also it is found that the rotations are nearly (65% to 80%) the rotations of the same beam but without preflex.
- The load carrying capacity is higher for larger profiles than small profiles; this is due to the larger contact surface between the flange and the concrete encasement which is led to an increasing in the contact surface (bond area) between the steel section and the encased concrete and also by the lower shortening of the concrete due to the shrinkage. The confinement effect of the steel profile in some areas of the concrete also increases the load carrying capacity. When reinforcing bars and headed shear studs are combined to provide the composite action, the longitudinal shear force transfer occurred mainly by friction forces acting at the interface among the concrete encasement and the structural steel.
- The values of strains at the steel-encased concrete surface (contact plane) for the models with full shear connection are nearly the same in comparison with the same model without shear studs were the strains values at the contact plane showing miner divergence.
- The finite element results show that the Poisson's ratio has insignificant effect on the increasing or decreasing the ultimate load of the composite encased beams.

NOTATIONS:

1-D	One Dimensional Mode
2-D	Two Dimensional Mode
3-D	Three Dimensional Mode
Ec	Modulus of Elasticity of Concrete
Es	Modulus of Elasticity of Steel
f	Function
f'_c	Uniaxial Compressive Strength of Concrete
f_t	Uniaxial Tensile Strength of Concrete
P	Applied Concentrated Load
ε	Strain
ε_{cu}	Ultimate Strain
ν	Poisson's Ratio
τ	Shear Stress
φ_s	Secant Angle
Δ_p	Cambering Produced in the Steel Section
Δ	Deflection
y	Distance from the Steel Section Centroid to the Top Surface of Compression Plange
I	Moment of Inertia
M	Bending Moment

REFEENCES:

- Yousif S. J., " Nonlinear Analysis of Composite Preflex Steel Beams Encased in Concrete", M.Sc., Thesis, University of Baghdad, Iraq, 2008.
- Airil Y. Mohd Yassina, and David A. Nethercotb, "Cross-Sectional Properties of Complex Composite Beams", Engineering Structures, Vol. 29 , 2007, pp.212–195 .
- "Steel-Concrete Composite Construction Using Rolled Sections"ARCELOR Sections Commercial S.A., Web-site:www.sections.arcelor.com, January-2005.
- Silvana De Nardin, and Ana Lucia H.C. El Debs, "Study of Partially Encased Composite Beams with Innovative Position of Stud Bolts"Journal of Constructional Steel Research, March-2008, pp.1–9 .
- Eurocode1994: Design of Composite Steel and Concrete Structures- Part 1-1: General rules And rules for buildings, English version, September 2002.
- **[**N. Roussel, S. Staquet, L. D'Aloia Schwarzentruber, R. Le Roy, and F. Toutlemonde, "SCC Casting Prediction for the Realization of Prototype VHPC-Precambered Composite Beams", Materials and Structures, Vol. 40, 2007, pp.877–887 .
- Josef Hegger, and Clause Goralski, "Structural Behavior of Partially Concrete Encased Composite Sections with High Strength Concrete", Composite construction in steel and Concrete, 2006, pp.346–355 .
- Swanson Analysis Systems, ANSYS. Online manual, version10.0 (2005) and Theory Reference.10th ed. Swanson Analysis Systems, s.1., s.d.
- Method of Manufacturing Preflex Beams", World Intellectual Property Organization (International Bureau), International Publication Number: WO 01/18319 A1, International Publication Date: 15 March 2001, pp 1-56.
- F.D. Queiroza, P.C.G.S. Vellascob, and D.A. Nethercota, "Finite Element Modeling of Composite Beams with Full and Partial Shear Connection", Journal of Constructional Steel Research, Vol.63, 2007, pp.505–521.